NJC

Accepted Manuscript

This is an *Accepted Manuscript*, which has been through the Royal Society of Chemistry peer review process and has been accepted for publication.

Accepted Manuscripts are published online shortly after acceptance, before technical editing, formatting and proof reading. Using this free service, authors can make their results available to the community, in citable form, before we publish the edited article. We will replace this *Accepted Manuscript* with the edited and formatted *Advance Article* as soon as it is available.

You can find more information about *Accepted Manuscripts* in the Information for Authors.

Please note that technical editing may introduce minor changes to the text and/or graphics, which may alter content. The journal's standard Terms & Conditions and the Ethical guidelines still apply. In no event shall the Royal Society of Chemistry be held responsible for any errors or omissions in this *Accepted Manuscript* or any consequences arising from the use of any information it contains.

ROYAL SOCIETY OF CHEMISTRY

www.rsc.org/njc

New Journal of Chemistry RSCPublishing

ARTICLE

Hydrogenation of NO and NO_2 over palladium and platinum nanocrystallites: case studies by field emission techniques

Cite this: DOI: 10.1039/xoxxoooooox

Received ooth January 2012,
Accepted ooth January 2012

DOI: 10.1039/xoxxoooooox

www.rsc.org/

C. Barroo,[a] S. V. Lambeets,[a] F. Devred,[a] T.D. Chau,[a] N. Kruse,[a] Y. De Decker,[b,c] and T. Visart de Bocarmé[a]

In this work, we investigate the catalytic hydrogenation of NO over palladium and platinum and of NO_2 over platinum surfaces. Samples are studied by field emission techniques including field emission/ion microscopies (FEM/FIM). The aim of this study is to obtain detailed information on the non-linear dynamics during NO_x hydrogenation over nanocrystallites at the atomic scale. The interaction between Pd and pure NO has been studied between 450 K and 575 K and shows the dissociative adsorption of NO. After a subsequent addition of hydrogen in the chamber, a surface reaction with the oxygen-adlayer can be observed. The phenomenon is reversible upon variation of the H_2 pressure, exhibits a strong hysteresis behaviour but does not show any unstable regime when control parameters are kept constant. On platinum, NO is dissociated and the resulting O(ads) layer can also react with H_2. Although occurring on both Pd and Pt metals, the reaction mechanism seems different. On palladium, NO dissociation takes place on the whole visible surface area leading to a "surface oxide" that can be reacted off by raising the H_2 pressure whereas on Pt, the catalytic reaction is self-sustained and restricted to <001> zone lines comprising {011} and {012} facets and where self-triggered surface explosions are observed. Two kinetic phase diagrams were established for the NO-H_2 reaction over palladium and platinum samples under similar experimental conditions. Their shapes reflect a different chemical reactivity of metal surfaces towards oxygen species resulting from the dissociation of NO.

NO_2 hydrogenation is followed over Pt samples and shows self-sustained kinetic instabilities that are expressed as peaks of brightness that are synchronized over the whole active area (corresponding to the <001> zone lines as in the NO case) within 40 ms, the time resolution of the video-recorder used for this work.

New Journal of Chemistry RSCPublishing

ARTICLE

A. Introduction

Nitrogen oxides (NO_x) emissions from vehicles are a matter of concern for the public health. NO_x abatement is highly desirable but the development of viable solutions still represents a major challenge for catalysts makers, especially in the growing market of lean-driven vehicles. NO is known to be oxidized to NO_2 under lean-burn conditions in automotive engines, and subsequently converted into N_2 in the presence of reducing species. The most investigated way to convert NO_x to N_2 in mobile sources is based on the concept of NO_x storage and reduction: NO_x are stored over the catalyst and reduced by a programmed transient excursion of the air/fuel ratio towards reducing conditions.

At the molecular level, a deep understanding of the mechanisms, kinetics and active sites of catalysts is mandatory to develop more efficient formulations. Surface science methods have been widely used to unravel fundamental features of the so-called deNOx catalysis over model surfaces, such as the adsorption energies of NO_x species at various coverages, adsorption geometries, kinetics of decomposition and recombination. The conditions under which these methods are used are far from those encountered in real catalytic applications. The well-known "pressure- and materials-gaps" are the subject of a number of studies that are aiming to bridge them.

Considering a real catalyst as a dispersion of nanoparticles over a support of high specific surface area, the ultimate goal is to identify the instant structure and composition of the surfaces during their ongoing catalytic activity. The approach of this work is to consider the extremity of a sharp metallic tip as a hemisphere, the size and shape of which are close to those of a single catalytic particle. Field emission methods are suitable to image them with atomic resolution and to follow their catalytic activity with nanoscale lateral resolution.

B. Experimental section

In a first set-up, video-Field Electron and Field Ion Microscopy (FEM/FIM) are used to image the surface structure of either a clean or an adsorbate-covered catalyst conditioned as a single nano-sized palladium or platinum 3D particle with a hemispherical shape. The instrument can be operated under truly *in-situ* reaction conditions. In order to investigate the modifications of the surface composition when the reaction proceeds, short field pulses of variable amplitude are applied under continuous supply of the gaseous reactants. Field pulses lead to the ionic desorption of the adsorbed layer. The respective ions are injected into a time-of-flight mass spectrometer. Structural changes of field emitter crystals are studied by FIM. Videos are acquired with a high-sensibility camera at a frame rate of 25 images per second.

Pd tips are electrochemically etched in a suspended drop of 10% aqueous solution of KCN at 3 V_{DC} from a high purity wire (Ø ~ 0.1 mm). The long durations necessary for etching – several tens of minutes – and the toxicity of KCN led us to designing a cathode so as to (i) allow an extended electropolishing duration without having to refresh the solution and to (ii) avoid the perturbation of the regular etching by the bubbles produced inside the droplet (see reference [1] for details). Platinum tips are etched in a molten salts mixture of NaCl and $NaNO_3$ (1:4 w/w). Samples are characterized by field ion microscopy (FIM). Cycles of thermal annealing, Ne^+ ion sputtering and field evaporation are used to clean the tips. The tip holders are built to allow the samples to be heated resistively. Temperatures can be accurately measured by a Ni/NiCr thermocouple at the basis of the tip and controlled between 50 K and ~1000 K. Figure 1a shows a field ionisation micrograph of a platinum sample resulting from the described preparation procedure. Assuming a hemispherical shape, net plane counting between known orientations on the field ion micrograph provides an estimation of the radius of curvature (R_c). As Pd shows identical crystallographic features, it is not presented here. A ball model with the shape of a hemisphere serves as a guide-to-the-eye to indicate that the most protruding sites are those above which field ionization preferentially occurs [2].

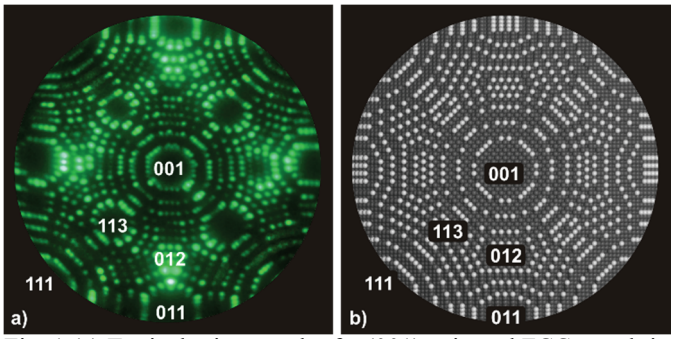

Fig. 1 (a) Typical micrograph of a (001)-oriented FCC metal tip sample imaged at high resolution by field ion microscopy (F = 35 V nm^{-1}, T = 40 K, P_{helium} = 10^{-3} Pa, R_c ~15 nm). (b) Ball model depicting the field ion micrograph.

All the pressures mentioned here are measured by means of a Bayard-Alpert ion gauge. The partial pressures are established in the vessel by a dynamical equilibrium controlled through independent leak valves. The chamber is constantly evacuated by a turbomolecular pump ensuring that chemical systems are kept far from their thermodynamic equilibrium. Values of partial pressures are corrected for each species considering the gas correction factors and the purity of the gas is checked by quadrupole mass spectrometry.

C. Results

C.1. FIM study of the NO-H_2 reaction over palladium nanocrystallites: hysteresis effects.

We first describe the effects of the adsorption of nitric oxide (NO) over palladium tips as followed by FIM and the influence of the presence of added hydrogen at well-defined P_{NO}/P_{H_2} pressure ratios. Strong hysteresis effects are observed but kinetic instabilities are not detected. In this paper, we use the "kinetic instabilities" as a generic term that comprises self-triggered modifications of the kinetic features that are observed or measured over one region on interest of the catalyst. Examples of kinetic instabilities are surface explosions occurring in a random or in an oscillatory manner. Bistable behaviour, where the chemical system undergoes a transition from one surface composition, *e.g.* metallic, to another, *e.g.* oxidized, without modification of the external control parameters is also an example of kinetic instability. The details of the experimental procedure aiming at determining hysteresis effect over field emitter tips have been described earlier [3]. Briefly, the tip

temperature is raised to values of interest (≈400–600 K) and pure NO is introduced at pressures from 10^{-4} to 10^{-2} Pa. The tip voltage is raised so as to develop an electric field of approximately 10 V nm^{-1} at the tip apex to produce a visible field ion pattern. Finally, hydrogen is slowly introduced at pressures between 10^{-4} and 10^{-2} Pa while continuously monitoring the pattern sequences using the video system. Figure 2 presents the overall brightness measurement during the interaction of a NO/H_2 gas mixture over a Pd tip at 450 K in the presence of a viewing field of +9 V nm^{-1}. The pressure of NO is kept constant at 10^{-3} Pa. Two micrographs obtained from a video sequence during that experiment are inserted in the figure. The snapshot corresponding to the step "1" illustrates the appearance of bright patterns which do not show any correlation with the underlying structure. Identical micrographs are observed in the presence of pure oxygen on Pd, and are also very similar to those observed in the presence of oxygen over rhodium under similar temperature and pressure conditions [4,5].

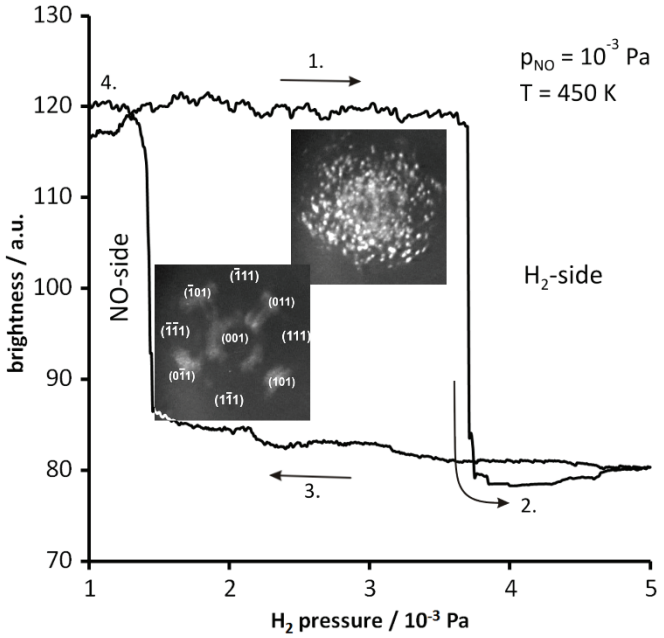

Fig. 2 Hysteresis measured during the NO-H_2 interaction over a (001) oriented Pd tip sample imaged by field ion microscopy (F = +9 V nm^{-1}, T = 450 K, P_{NO} = 10^{-3} Pa, R_c ~15 nm). The surface oxide appears bright and is abruptly reacted off when P_{H_2} exceeds a threshold value.

The NO molecule undergoes dissociation into N(ads) and O(ads). It is most likely that the resulting O(ads) subsequently diffuses below the surface. This interpretation is in good agreement with a number of studies over various Pd single crystal surfaces. Temperature programmed desorption [6,7] and ion scattering spectroscopy [8] provide direct evidences of the presence of oxygen below the first layer upon adsorption of oxygen containing species. In the current study, dissociative adsorption of NO on Pd seems to occur on the whole visible surface area and forms a surface oxide without significant preference for any particular facet. Interestingly, a drastically different behaviour is observed over platinum tips as will be described in section C2. Increasing the H_2:NO ratio to 3.6 causes a fast decrease of the overall brightness. As the ionisation potential of NO is rather low (IP=9.3 eV) and lower than the one of H_2 (12.6 eV), as well as those of possible reaction products, H_2O (12.6 eV), N_2 (14.5 eV) and NH_3 (10.07 eV), NO^+ is the main species responsible for image formation by FIM. Any change of the brightness must then be attributed to a variation of the ionisation probability of the NO molecule as a consequence of compositional changes of the Pd surface.

In the resonance field ionisation model introduced by Kreuzer and Wang, an oxygen-covered Pd surface appears brighter than a hydrogen-covered one when using NO as imaging gas [9]. Besides this, the trend follows the simple ionisation model introduced by Müller that predicts a higher ionisation probability above surfaces with higher work function [2]. The surface oxidation of palladium has also been proven by different methods under similar experimental conditions [10-13]. The abrupt change in brightness is therefore consistently interpreted as being due to the transition from an NO- and oxygen- (and, possibly, nitrogen-) covered Pd surface to an essentially hydrogen-covered one. Under the reported experimental conditions, it may be advanced that the recombination of two N(ads) towards molecular N_2 is in operation. Its fast desorption as a stable neutral species with a higher ionization potential makes its detection ineffective. For the sake of clarity, we will address the system as being in the "hydrogen side" under these conditions.

As long as the hydrogen pressure is kept above the value necessary to trigger the transition to the hydrogen side, the system remains stable without direct evidence for the occurrence of a surface reaction. Water formation cannot be excluded however if we consider that the electric field that is necessary to ionize water molecules is above 10 V nm^{-1} [12,13]. Decreasing the H_2:NO ratio from 5 to 2 enhances the local brightness along the <100> zones line between the periphery of the topmost (001) facet and the peripheral {011} facets, as shown by the bottom inset in Figure 2. It is possible that, under the experimental conditions corresponding to the state of low brightness (steps 2 and 3 in Figure 2), H(ads) diffuses under the surface. This behaviour is in accordance with the well-known dissolution of hydrogen in bulk Pd. A further decrease of the H_2:NO ratio to 1.4 (step 4) causes a sudden increase of the overall brightness towards values similar to those encountered in step 1. This is understood as being due to preferential NO adsorption and dissociation. Subsequent subsurface penetration of the O(ads) species likely influences the image brightness. Under these conditions, the system is in its "NO-side". H_2 partial pressure is too low to trigger the reduction of the surface oxide leading back to the hydrogen side. The observations are remarkably repeatable and do not depend on the rate at which the hydrogen partial pressure is increased or decreased.

Figure 2 demonstrates the presence of a hysteresis effect. With constant NO partial pressure, the transition from a bright to a dark pattern and vice-versa depends on whether the hydrogen partial pressure is increased or decreased. The effect is significant at lower temperatures, whereas the hysteresis narrows with higher temperatures. It also shifts towards lower H_2:NO ratios. A kinetic phase diagram has been established for temperatures between 450 K and 575 K and is shown in Figure 3 for a constant field strength of +9 V nm^{-1}. We notice the intentional use of the term "kinetic phase diagram", which is used by analogy to equilibrium thermodynamics although the observed transitions occur between different states that are kept far from thermodynamic equilibrium and that are thus of kinetic nature. The appearance of kinetic features is related from this point of view to the appearance of different reactive surface states that are in competition [14]. Symbols ◆ and ▪ indicate hydrogen pressure above and below which no visible change of the pattern is observed within 15 minutes, respectively. Relative error bars on this logarithmic plot are calculated on the basis of a minimum of five experiments per point.

The existence of the hysteresis region can only be established within the indicated range of temperatures, i.e. 450–575 K. Below 450 K the total pressure limit is set by the difficulty of satisfactorily reproducing the phenomenon, and image interpretation is difficult because of the decreasing overall image brightness. This may be explained by the absence of NO dissociation at lower temperatures, which is consistent with earlier studies on flat and stepped surfaces [7,15]. Above 575 K, indications for the occurrence of field evaporation arise for

extended durations of back-and-forth variations of the H_2 partial pressure. This compromises the correct definition of the surface in the context of the present study. We also notice that the temperature dependence over the hysteresis behaviour was investigated in random order so as to avoid the possible emergence of memory effects when increasing or decreasing the temperature systematically.

In FEM studies of the NO-H_2 reaction over Pd tips, Cobden *et al*. observed a considerable change of the emission patterns at 500 K in the presence of NO gas [16]. They suggested that this temperature marks the transition from molecularly adsorbed NO to atomic N(ads) and O(ads) species. Quite generally, the sudden transformation of structures is observed for all measured temperatures during the decrease or increase of the hydrogen pressure, while being on one of the two branches of the hysteresis region. A further approach to a possible bifurcation point leading to kinetic oscillations has not been possible because of the described technical reasons.

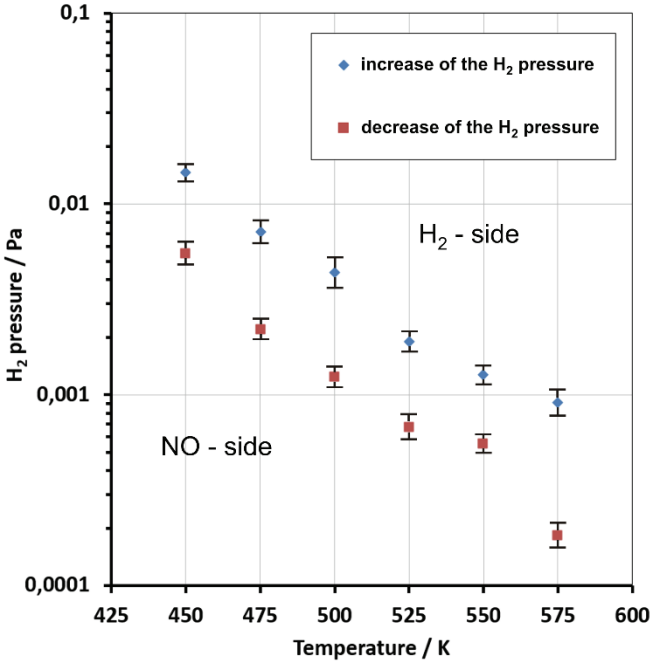

Fig. 3 Kinetic phase diagram of the NO-H_2 reaction over the Pd crystal presented in Fig 2. $F = +10$ V nm^{-1}.

From the presented data, the processes seem not to be limited to the surface but rather to involve the subsurface region as well. By contrast to similar chemical systems such as NO-H_2/Pt or H_2-O_2/Rh [4], the NO-H_2/Pd is quite unique in that the hysteresis region does not exhibit any sign of kinetic instability, such as excitability or oscillations. If the conditions are set to the region of hysteresis, the system keeps the features of the side from which it has been driven and it does not fluctuate substantially. In this particular case, we suggest that the exchange of hydrogen atoms between the palladium surface and the bulk, H(ads) → H(bulk), is in operation on the hydrogen side of the reaction system but is partly inhibited on the NO side. Over the years, a lot of research has been undertaken on the interaction between H_2 and Pd [17-20]. Hydrogen adsorbs and dissociates even at 90 K and can diffuse into the bulk at room temperature, a feature that is industrially applied for the purification of hydrogen gas by palladium diffusers. Interestingly, it was found that water is produced by the reaction between O(ads) and H(bulk) and, although much less so, between O(ads) and H(ads) [21]. In the present case, the electric field enhances the surface oxidation in a similar way to that of rhodium [13]. A careful analysis of the formation of the surface oxide indicates that it forms from the topmost (001) plane towards the periphery of the tip. Interestingly, this progression is rather fast – a few tenths of second – but stops before the limits of the imaged surface area of the tip characterized with high resolution at low temperature. It is then most probable that the tip shank remains metallic when the apex is covered by a surface oxide when the system is in its NO-side. Figure 4 shows a scheme depicting the situations encountered in the hydrogen side (left) and in the NO-side (right).

High-resolution data by atom-probe probe analyses during the ongoing processes are necessary to support this conclusion. Since the field evaporation hinders the determination of the bifurcation point above 575 K, further experiments will be performed at somewhat lower static fields and possibly in its absence. In the latter case, field pulses will serve to rupture surface species for mass analysis without simultaneous FIM imaging.

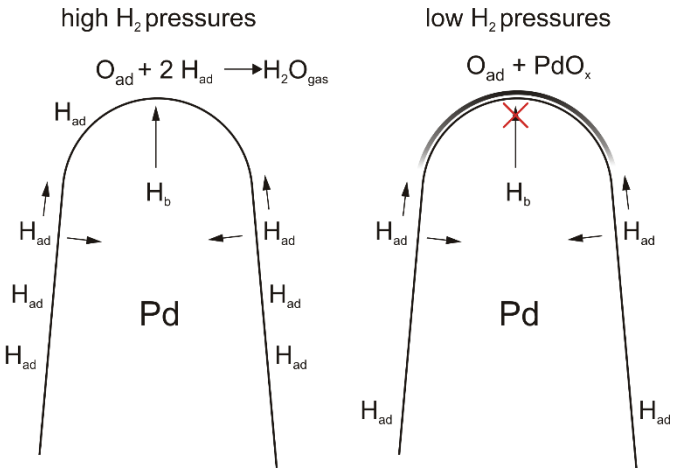

Fig. 4 Schematic representation of the advanced reason for the absence of instabilities of the NO-H_2/Pd system within its hysteresis region. The surface oxide at the tip apex hinders the mobility of the hydrogen atoms and limits its supply from the bulk (H(bulk)) to the surface.

C.2. FIM study of the NO-H_2 reaction over platinum nanocrystallites: hysteresis and excitability.

A similar procedure was applied for the NO-H_2 reaction over platinum. Starting from a clean sample similar to that of Figure 1b with a radius of 7.5 nm, neon gas is evacuated, the field is set to zero, the Pt tip is then heated to 450-530 K and a mixture of NO/H_2 is introduced in the chamber. Upon increase of the electric field, a field ion pattern appears. Rapid ignition phenomena of the catalytic NO reduction are seen and the main features of such "surface explosions" are shown in Figure 5 under the experimental conditions mentioned in the caption. Starting with a rather dim image in Figure 5a, kink sites sitting over the {011} layer edges of the <100> zone suddenly turn bright in Figure 5b. The brightness immediately extends towards the (001) pole (Figure 5c-d). After about 160 milliseconds, the high brightness decreases to a field ion pattern identical to Figure 5a. The same sequence of reactive patterns may repeat after several seconds but the ignition of the surface explosions cannot be predicted. Accordingly, durations between two surface explosions are not well defined and vary from a few seconds to some minutes.

The influence of the tip radius over the emergence of the surface explosion has been addressed by Chau *et al*. [23,24] who provided evidences that the reaction is triggered along the <001> zones lines. The latter have the particularity to cover facets which expose atoms in the half-crystal position. More precisely, the distance between two atoms in kink site positions in the

perpendicular direction to <001> zone lines corresponds to the lattice parameter, 0.392 nm for Pt.. Nitric oxide dissociative adsorption is known to be promoted by steps. Although a Pt(210) single-crystal surface shows high dissociation activity [25], a (111) surface, even stepped, remains inactive [26-28] so that catalytic water formation does not occur. Our FIM results are in line with these data. We also performed atom-probe measurements close to the (001) pole and found that NO^+ was dominating the mass spectra under all conditions (not shown here), which indicates that this species is responsible for the image formation. Intensity spikes of short duration were also observed, suggesting the occurrence of NO(ads) surface diffusion. The simultaneous appearance of H_2O^+/H_3O^+ species proves water formation to be in operation. Quite interestingly, PtO_x^{n+} ions appear at somewhat high field strengths. The extent to which a (reversible) surface oxidation is involved in the fluctuating surface reaction must await further experiments, however.

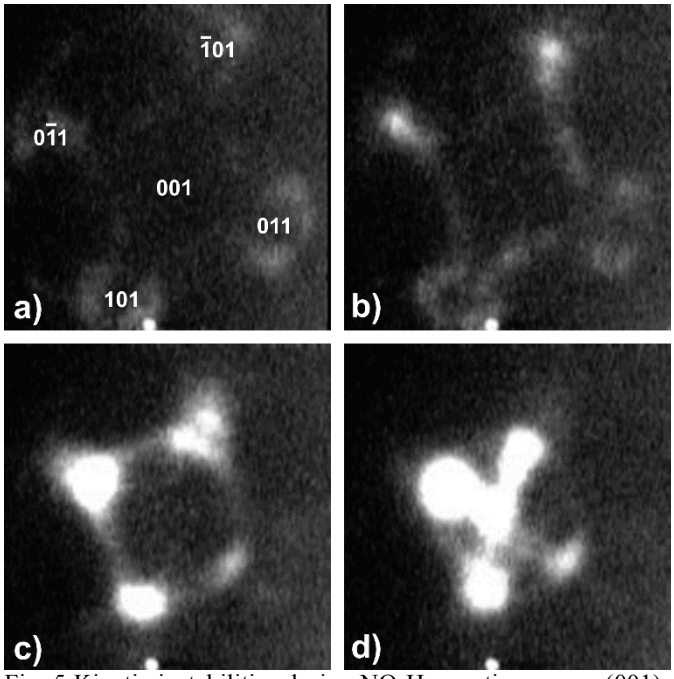

Fig. 5 Kinetic instabilities during NO-H_2 reaction over a (001)-oriented Pt field emitter tip. T = 525 K, P_{NO} = 2.5×10^{-3} Pa, P_{H_2} = 2.0×10^{-3} Pa, R_c ~ 9 nm. The reaction is triggered within 40 ms near the four {011} facets and propagates along <001> zone lines towards the (001) pole within 200 ms.

A kinetic phase diagram has been established as well for the NO-H_2 reaction over platinum tips following the same procedure as described in section C1 for the Pd case. As the phenomenology of the surface reactions is readily different for the two metals, we associate here the H_2- and NO-sides to states of low reactivity. Above 480 K, a region of the diagram develops where kinetic instabilities are observed. Above 510 K, the kinetic instabilities are observed over an even larger range of H_2 pressures but are not presented in Figure 6 because of a lack of repeatability in the measurements. Interestingly, when reducing the H_2 pressure drastically down to ~10^{-5} Pa the same ignition phenomena were observed. We conclude that the H(ads) reservoir on the Pt surface is still large enough under these conditions to allow for surface diffusion and ignition of the oxygen clean-off reaction. In analogy with the O_2-H_2/Rh system [4], we consider that not only the apex region but also (and mainly) the shank acts as H(ads) supply reservoir. Since the occurrence of repeated ignition phenomena is not significantly affected upon variation of the H_2 pressure, supply by H(ads) diffusion cannot determine the time between two surface explosions

A theoretical treatment of the role of fluctuations and spatial correlations in the emergence of bistability and surface explosion has been proposed for a minimal model of the system under consideration [29]. The authors demonstrate that rapid catalytic ignition is possible in the presence of fluctuations of composition, which become important for systems of nanometric sizes. A more realistic model was developed since then, showing that the observed phenomena can be seen as a fluctuation-induced intermittency related to the intrinsically excitable character of the reaction [29].

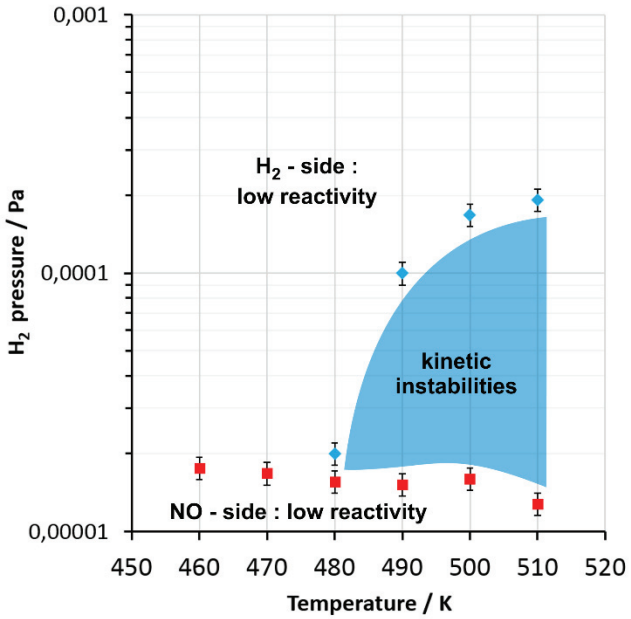

Fig. 6 Kinetic phase diagram of the NO-H_2 reaction over platinum. P_{NO} = 10^{-3} Pa, F = +9 V nm^{-1}

C.3. FEM study of the NO_2-H_2 reaction over platinum nanocrystallites: kinetic oscillations.

This section addresses the catalytic reduction of NO_2 over platinum field emitter tips by means of Field Emission Microscopy (FEM). By contrast to FIM, the tip is negatively polarized and field-emitted electrons are responsible for image formation. The experimental procedure is similar to that described in section C2. During the reaction, temperature, field and pressure of both gases are fixed. The modulations of brightness during the ongoing catalytic process translate the variations of the local work function that is itself affected by the modifications of the surface composition. The study of dynamics taking place on a single grain of catalyst is achieved by a careful analysis of the brightness signal.

Just like for the NO-H_2/Pd and Pt systems, the first proof for a nonlinear character of the NO_2-H_2/Pt system is the existence of a hysteresis loop. The latter will be detailed in a forthcoming article. Self-sustained surface explosions are observed in both FEM and FIM modes. Kinetic instabilities were found to persist with similar pattern formation when reversing the polarity. Characteristic times under oscillatory conditions changed however due to variations in the gas supply function. With a careful control of the parameters, we can observe transitions between two distinct regimes characterized by different levels of brightness. A regime of low brightness is associated with a surface covered by oxygen resulting from the dissociative adsorption of NO_2 on Pt. O(ads) species over Pt are notoriously known to increase the local work function [31]. A regime of high brightness is associated with a metallic surface covered by hydrogen. The reaction between O(ads) and H(ads) produces

water, which decreases the work function of electrons over Pt. The observation of water production is made when a transition from O-covered surface to H-covered surface occurs: a peak of higher intensity is present. Figure 7 shows a snapshot of a digitized video sequence of the field emission pattern when this transition occurs. Some of the Miller indices are indicated by circles that correspond to regions of interest (ROI). The mean brightness inside these regions is monitored using the open-source software "Tracker" [32]. Time series of these ROIs are presented in Figure 8. To account for the subtle variations of the sensitivity of the camera with respect to sudden variations of the total brightness of the monitored picture, a second ROI has been chosen over a region that is outside the imaged area of the tip sample. This actually monitors the total dark current of the recording device and of the screen of the microscope.

The transitions between the oxygen-rich and the hydrogen-rich states are also supposed to find their roots in the stochastic fluctuations of the local composition of the surface. It is interesting to notice how similar these observations are compared to those obtained with $NO-H_2$ mixtures by FIM. For the two systems, all the {011} facets ignite simultaneously within the time resolution of the video-recorder (40 ms) whereas the reaction does not propagate toward the central (001) pole in the current case. According to Figures 7 and 8 the high catalytic activity is rather intense over {011} facets and restricted to the <001> zone lines. The peripheral {111} and {113} planes of the crystal do not participate, as can be concluded from the profiles of the (111) and (113) time series, which are practically identical to that of the background noise. Interestingly, the higher activity of planes along <001> lines is in qualitative agreement with reports on the catalytic activity of the $NO-H_2$ reaction over macroscopic platinum single crystals [33,34].

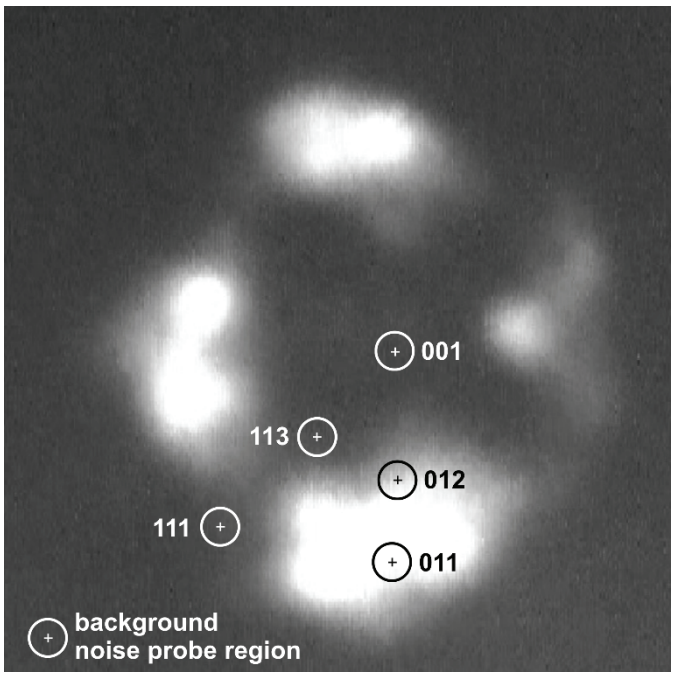

Fig. 7. NO_2-H_2 reaction over platinum imaged by field emission microscopy. The snapshot is taken when the reaction ignites over the {011} facets. A number of regions are shown and their instant brightness is monitored (see Fig. 8). $P_{NO_2} = 10^{-3}$ Pa, $P_{H_2} = 10^{-3}$ Pa, $T = 390$ K, $R_c \sim 18$ nm

This can also be highlighted on Figure 8. Although the brightness analysis cannot be used as a quantitative way to monitor the water production, it highlights the qualitative activity of various facets that are in communication with each other. Indeed, the variation of brightness for the (011) facet between the O-covered surface and H-covered surface is more intense as compared to the (012) and (001) facets. It is important to note that the (001) facet starts to exhibit catalytic activity after a time delay of some minutes. Under these conditions, patterns obtained for the NO_2-H_2 reaction are similar to that of Figure 5d captured during the $NO-H_2$ interaction over Pt. Still, wave propagation is not observed with the time resolution of 40 ms and all the active facets ignite simultaneously. The increased activity of the (001) topmost layer is attributed to the occurrence of a morphological reconstruction of the tip apex from a quasi-hemisphere toward a polyhedron. This reconstruction is well documented and has been reported after having dosed NO over Pt field emitter tips at $T = 525$ K [35].After this reconstruction, peaks appear with a more regular frequency. A careful assessment of this transition and the associated regular oscillations is currently under progress. One of the most striking features of these time series is the rigorous synchronisation of the process on all the active facets. The sharp increase in the brightness signal spans a relatively short time scale (120 ms), meaning that the underlying process governing the water production is fast, comprises a strong spatial coupling, and should be identical for all facets. The rate of water formation via the reaction between O(ads) and H(ads) is limited by the addition of the first hydrogen [36], thus once OH(ads) is formed, the further addition of H(ads) is supposed to be fast. The synchronisation of the reaction over the whole active catalyst suggests that the hydrogen species are in constant dynamical equilibrium at the surface and diffuse over the whole tip. Further experiments are currently under investigation to fully understand the mechanism of this reaction, and the role played by the different species involved. Tentative mechanisms have been proposed earlier to describe the non-linear kinetic behaviours of the systems reported in this paper. Although realistic, these assumptions suffer from a lack of a direct local chemical analysis during the ongoing reactions and are thus subject to discussions [37]. Using field pulses, atom probe methods have been used in our group with success to follow the kinetics of a number of surface reactions [38-40]. Systematic atom analyses on the NO_2-H_2/Pt system will be addressed to determine the evolutions of the surface composition over regions of interests and to unravel the role of NO(ads) species in the progress of the reaction.

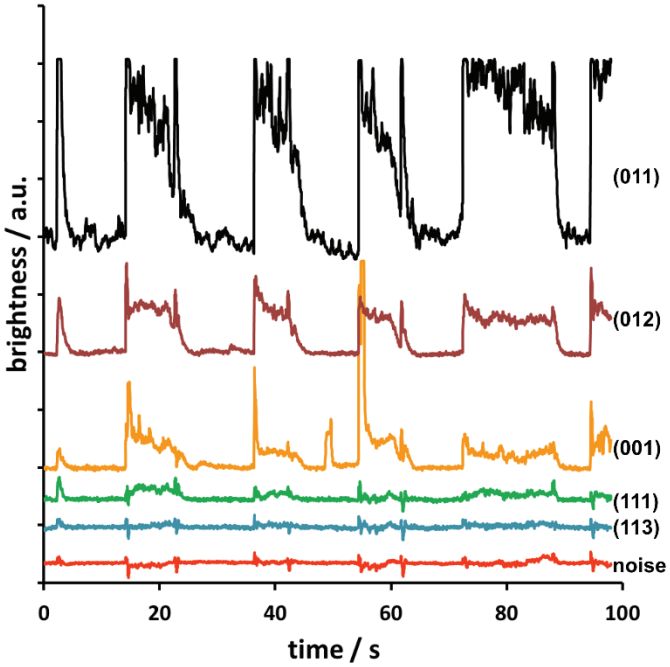

Fig. 8 Time series of the local brightness encountered during NO_2-H_2 reaction over Pt. $P_{NO_2} = 10^{-3}$ Pa, $P_{H_2} = 10^{-3}$ Pa, $T = 390$ K.

Conclusions

The reported case studies show that the field electron (FEM) or the field ion microscope (FIM) can be used as an *in situ* reactor where catalytic surface reactions are observed in the 10^{-5}-10^{-2} Pa pressure range. Due to its specific size and morphology, a tip apex models a single catalytic nanoparticle made of an ensemble of facets of different crystallography that are in communication with each other.

Hysteresis effects were observed for the NO-H_2 reaction over Pd without self-triggered transitions from the metallic state and vice-versa within the hysteresis region. It is advanced that the Pd surface oxide reduces the mobility of dissolved hydrogen atom from the bulk to the tip apex making its reduction possible only for high values of the external H_2(g) pressure. Self-sustained kinetic instabilities were observed for the catalytic NO-H_2 and NO_2-H_2 reactions over platinum. The phenomenology of these two systems is remarkably similar, although they have been studied with FIM and FEM respectively and thus in the presence of opposite electric field vectors. Facets lying along the <001> zone-lines comprising {011}, {012} and the (001) planes are the most active whereas {111} and {113} facets do not show signs of catalytic activity. The fast and simultaneous ignition of the facets suggests a strong spatial coupling.

The presented methods allow one to study ongoing catalytic reactions with a nanometric lateral resolution. This represents a necessary step for the understanding of the behaviour of supported metal catalysts having active nanocrystallites of the same size. In that respect, they partially fill the gap between surface science approaches and applied catalysis. The experimental data they provide can lead to new insights for the development of theoretical concepts of heterogeneous catalysis but also call for systematic studies with atom-probe methods so as to quantify in a direct way the evolution of the local surface compositions with time.

Acknowledgements

C.B. (FRS Research fellow) and T.D.C. thank the Fonds de la Recherche Scientifique (F.R.S.-FNRS) for financial support (PhD grants from FNRS and FRIA respectively). The authors gratefully thank the Van-Buuren Foundation for a financial support for the acquisition of equipment and the Wallonia-Brussels Federation (Action de Recherches Concertées n°AUWB 2010-2015/ULB15). The authors also thank Prof. Pierre Gaspard for fruitful discussions regarding the data processing of the non-linear kinetics behaviours reported in this article.

Notes and references

[a] Université Libre de Bruxelles, Faculty of Sciences, Chemical Physics of Materials, CP243, 1050 Brussels, Belgium.

[b] Université Libre de Bruxelles, Faculty of Sciences, Non Linear Physical Chemistry Unit, CP231, 1050 Brussels, Belgium.

[c] Université Libre de Bruxelles, Faculty of Sciences, Interdisciplinary Center for Nonlinear Phenomena and Complex Systems (CENOLI), 1050 Brussels, Belgium.

1 T. Visart de Bocarmé, M. Moors, N. Kruse, I. S. Atanasov, M. Hou, A. Cerezo and G. D. W. Smith, *Ultramicroscopy*, 2009, **109,** 619.

2 E.W. Müller and T. T. Tsong, *Field ion microscopy, principles and applications*, Elsevier, New York (NY), 1969.

3 T. Visart de Bocarmé and N. Kruse, *Ultramicroscopy*, 2011, **111,** 376.

4 J.-S. McEwen, P. Gaspard, T. Visart de Bocarmé and N. Kruse *Proc. Natl. Acad. Sci. U. S. A.* 2009, **106**, 3006.

5 V. K. Medvedev, Y. Suchorski, C. Voss, T. Visart de Bocarmé, T. Bär and N. Kruse, *Langmuir*, 1998, **14**, 6151.

6 I. Nakamura, T. Fujitani and H. Hamada, *Surface Sci*. 2002, **514**, 409.

7 R. G. Sharpe and M. Bowker, *Surface Sci*. 1996, **360**, 21.

8 W. S. Epling, G. B. Hoflund and D. M. Minahan, *Catal. Lett.* 1996, **39**, 179.

9 H. J. Kreuzer and L. C. Wang, *Z. Phys. Chem.* 1997, **202**, 127.

10 H. Conrad, G. Ertl, J. Küppers and E. E. Latta, *Surface Sci*. 1977, **65**, 245.

11 E. H. Voogt, A. J. M. Mens, O. L. J. Gijzeman and J.W. Geus, *Catal. Today*, 1999, **47**, 321.

12 E. M. Stuve, *Chem. Phys. Lett*. 2012, **519–520**, 1.

13 J.-S. McEwen, A. Garcia Cantu Rosa, P. Gaspard, T. Visart de Bocarmé and N. Kruse, *Catalysis Today*, 2010, **154**, 75.

14 M. Ehsasi, M. Berdau, T. Rebitzki, K. P. Charlé, K. Christmann and J. H. Block, *J. Chem. Phys*. 1993, **98**, 9177.

15 R. D. Ramsier, Q. Gao, H. Neergaard Waltenburg, K. W. Lee, O. W. Nooij, L. Lefferts and J. T. Yates, *Surface Sci.*, 1994, **320**, 209.

16 P. D. Cobden, B. E. Nieuwenhuys and V. V. Gorodetskii, *Appl. Catal. A*, 1999, **188**, 69.

17 H. Conrad, G. Ertl and E. E. Latta, *Surface Sci.*, 1974, **41**, 435.

18 T. Engel and H. Kuipers, *Surface Sci.*, 1979, **90**, 162.

19 W. Dong, G. Kresse and J. Hafner, *J. Mol. Catal. A*, 1997, **119**, 69.

20 T. Mitsui, M. K. Rose, E. Fomin, D. F. Ogletree and M. Salmeron, *Nature* 2003, **433**, 705.

21 T. Engel and H. Kuipers, *Surface Sci.* 1979, **90**, 181.

22 J.-S. McEwen, P. Gaspard, T. Visart de Bocarmé and N. Kruse, *J. Phys. Chem.* 2009, **113**, 17045.

23 T.D. Chau, T. Visart de Bocarmé and N. Kruse, *Surf. Interface Anal*. 2004, **36**, 528.

24 T. Visart de Bocarmé, T.D. Chau and N. Kruse, *Topics in Catal*, 2006, **39**, 111.

25 J.M. Gohndrone, Y.O. Park and R.I. Masel, *J. Catal.*, 1985, **95**, 244.

26 N. Kruse, G. Abend and J.H. Block, *J. Chem. Phys*., 1988, **88**, 1307.

27 T.H. Lin and G.A. Somorjai, *Surface Sci*., 1981, **107**, 573.

28 C.T. Campbell, G. Ertl and J. Segner, *Surface Sci*. 1982, **115**, 309.

29 Y. De Decker and F. Baras, *Eur. Phys. J. B*, 2010, **78**, 173.

30 Y. De Decker, T. D. Chau, F. Baras, T. Visart de Bocarmé, C. Barroo, and N. Kruse, *in preparation*.

31 P.T. Dawson and Y.K. Peng, *Surface Sci.*, 1980, **92**, 1.

32 D. Brown, Computer Program "*Tracker video analysis and modeling tool*", Version 4.80 (2009), WWW Document, (http://www.cabrillo.edu/~dbrown/tracker/)

33 C. T. Campbell, G. Ertl and J. Segner, *Surface Sci.*, 1982, **115**, 309.

34 J.M. Gohndrone,Y.O. Park and R.I. Masel, *J. Catal*. 1985, **95**, 244.

35 C. Voss and N. Kruse, *Appl. Surf. Sci.* 1995, **87-88**, 134.

36 A. Michaelides and P. Hu, *Journal of Chemical Physics*, 2001, **114**, 513.

37 V.V. Gorodetskii, V.I. Elokhin, J.W. Bakker, B.E. Nieuwenhuys, *Catal. Today*, 2005, **105**, 183.

38 M. Moors, H. Amara, T Visart de Bocarmé, C. Bichara, F. Ducastelle, N. Kruse and J.-C. Charlier, *ACS Nano*, 2009, **3**, 511.

39 N. Kruse, *Mater. Sci. Eng. A*, 1999, **270**,75.
40 N. Kruse and T. Visart de Bocarmé, in "*Handbook of Heterogeneous Catalysis*", 2nd edition, Eds. G. Ertl, H. Knözinger, J. Weitkamp, F. Schüth, Wiley-VCH (2008), pp.870-895.

